Drug Design, Development and Therapy

Dovepress
open access to scientific and medical research

Open Access Full Text Article

ORIGINAL RESEARCH

Integrated Network Pharmacology Analysis and Pharmacological Evaluation to Explore the Active Components and Mechanism of *Abelmoschus manihot* (L.) Medik. on Renal Fibrosis

This article was published in the following Dove Press journal:
Drug Design, Development and Therapy

Lifei Gu[1]
Fang Hong[1]
Kaikai Fan[1]
Lei Zhao[1]
Chunlei Zhang[1]
Boyang Yu[1,2]
Chengzhi Chai[1]

[1]Jiangsu Key Laboratory of TCM Evaluation and Translational Research, School of Traditional Chinese Pharmacy, China Pharmaceutical University, Nanjing 211198, People's Republic of China; [2]Research Center for Traceability and Standardization of TCMs, School of Traditional Chinese Pharmacy, China Pharmaceutical University, Nanjing 211198, People's Republic of China

Drug Design, Development and Therapy downloaded from https://www.dovepress.com/
For personal use only.

Background: Renal fibrosis is a common pathological outcome of chronic kidney diseases (CKD) that is considered as a global public health issue with high morbidity and mortality. The dry corolla of *Abelmoschus manihot* (L.) Medik. (AMC) has been used for chronic nephritis in clinic and showed a superior effect in alleviating proteinuria in CKD patients to losartan. However, the effective components and underlying mechanism of AMC in the treatment of renal fibrosis have not been systematically clarified.

Methods: Based on drug-likeness evaluation, oral bioavailability prediction and compound contents, a systematic network pharmacology analysis was conducted to predict the active ingredients. Gene Ontology, Kyoto Encyclopedia of Genes and Genomes pathway analysis and protein–protein interaction analysis were applied to predict the potential pathway and target of AMC against renal fibrosis. The formula of component contribution index (CI) based on the algorithm was used to screen the principal active compounds of AMC in the treatment of renal fibrosis. Finally, pharmacological evaluation was conducted to validate the protective effect and primary predicted mechanism of AMC in the treatment of renal fibrosis on a 5/6 nephrectomy mice model.

Results: Fourteen potential active components of AMC possessing favorable pharmacokinetic profiles and biological activities were selected and hit by 17 targets closely related to renal fibrosis. Quercetin, caffeic acid, 9.12-octadecadienoic acid, and myricetin are recognized as the more highly predictive components as their cumulative contribution rate reached 85.86%. The AMC administration on 5/6 nephrectomy mice showed a protective effect on kidney function and renal fibrosis. The hub genes analysis revealed that AMC plays a major role in inhibiting epithelial-to-mesenchymal transition during renal fibrosis.

Conclusion: Our results predicted active components and potential targets of AMC for the application to renal fibrosis from a holistic perspective, as well as provided valuable direction for further research of AMC and improved comprehension of renal fibrosis pathogenesis.

Keywords: *Abelmoschus manihot* (L.) Medik., network pharmacology, renal fibrosis, 5/6 nephrectomy, active components

Introduction

Chronic kidney disease (CKD) has increasingly become a global public health issue with high morbidity and mortality.[1] The alarming epidemiological data indicate CKD affects nearly 7~12% of the adult population worldwide.[2] Progressive development of CKD results in renal fibrosis, a situation characterized by inflammatory cell infiltration,

Correspondence: Chengzhi Chai; Boyang Yu
Jiangsu Provincial Key Laboratory for TCM Evaluation and Translational Development, China Pharmaceutical University, Nanjing, Jiangsu 211198, People's Republic of China
Tel +86 25 86185955
Fax +86 2586185158
Email chengzhichai@cpu.edu.cn; boyangyu59@163.com

submit your manuscript | www.dovepress.com
DovePress
http://doi.org/10.2147/DDDT.S264898

© 2020 Gu et al. This work is published and licensed by Dove Medical Press Limited. The full terms of this license are available at https://www.dovepress.com/terms.php and incorporate the Creative Commons Attribution – Non Commercial (unported, v3.0) License (http://creativecommons.org/licenses/by-nc/3.0/). By accessing the work you hereby accept the Terms. Non-commercial uses of the work are permitted without any further permission from Dove Medical Press Limited, provided the work is properly attributed. For permission for commercial use of this work, please see paragraphs 4.2 and 5 of our Terms (https://www.dovepress.com/terms.php).

tubular atrophy, as well as extracellular matrix production and deposition, which resulted in more serious renal function loss and kidney tissue deterioration.[3,4] Current treatment strategies can hardly reverse the progression of renal fibrosis. Accordingly, to seek for potential therapeutic drugs to slow or halt the development of renal fibrosis is urgently needed in this field. Recently, numerous cases demonstrated that natural products have been increasingly recognized as an alternative source for delaying the progress of renal fibrosis on account of the conventional experience and the multi-target characteristics.[5,6]

Abelmoschus manihot (L.) Medik. (*A. manihot*) is an annual or perennial herbal plant of folk medicine from the Malvaceae family. It was firstly recorded in Jiayou Materia Medica and has been used to treat inflammation-related diseases, including inflammation of the urinary system dating back to the Song dynasty. The extract of the dry corolla of *A. manihot* (AMC) is the main ingredient of Huangkui capsule, which is a Chinese patent medicine widely used for chronic nephritis in China. A prospective, multicenter randomized, controlled clinical trial has confirmed that AMC is effective in patients with CKD of stages 1–2, and shows better anti-proteinuria efficacy than losartan.[7,8] Pharmacological studies accordingly revealed the effectiveness of AMC on decreasing albuminuria, alleviating early glomerular injury[9] and inhibiting renal tubular epithelial-mesenchymal transition (EMT)[10] in different animal models like diabetic nephropathy rats, adriamycin-induced renal injury mice, etc. However, the underlying mechanism of AMC against renal fibrosis has not been clarified.

Network pharmacology is a new strategy based on the theory of systems biology, network analysis of biological systems, and the selection of specific signal nodes for multi-target drug molecule design.[11,12] It can save the research and development costs of drugs, and is increasingly becoming a novel research method commonly applied in traditional Chinese medicines (TCMs).[13,14] A number of reports have shown network pharmacology is a suitable method for the prediction of active components, molecular mechanisms, potential targets, and pharmacological interaction analysis of TCMs from a system perspective.[15]

Our study is the first to identify potential bioactive compounds in AMC and elucidate its mechanisms in renal fibrosis treatment by using the network pharmacology approach. We respectively collected the information of targets from active ingredients in AMC and targets of renal fibrosis from several databases. Furthermore, experiments in vivo were performed to confirm the protective effect of AMC on kidney function and renal fibrosis in the 5/6 nephrectomy mice model. Our results clarified the anti-fibrosis effect of AMC on a canonical CKD model and might provide a potential candidate for the treatment of renal fibrosis.

Materials and Methods

Chemical Components Database Construction

The chemical constituents of the AMC were systematically isolated and identified by our group in a previous study,[16] and then wide-scale text mining of PubMed (https://www.ncbi.nlm.nih.gov/pubmed/) and CNKI (http://www.cnki.net/) databases was performed to collect reported components in AMC.

Active Components Screening

An absorption, distribution, metabolism, and excretion (ADME) system was employed to select active components with favorable pharmacokinetics properties. In order to obtain compounds with higher oral absorption, utilization, and biological properties for further analysis, the active components from AMC were mainly filtered by integrating oral bioavailability (OB)[17] and drug-likeness (DL).[18] Based on the literature, OB≥30% and DL≥0.18 were set as the threshold values.[19,20] Besides, owing to the profound pharmacological effects and high contents, some compounds with high content and profound pharmacological effects were supplemented as the candidate compounds for further analysis.[21,22] Details of the selected components are summarized in Supplementary Table S1.

Component Targets of AMC

All active components were put into the PubChem Database (http://pubchem.ncbi.nlm.nih.gov/), a public repository for information on chemical substances and their biological activities,[23] to acquire the PubChem CID and canonical SMILES. The PubChem CID list was imported into BATMAN-TCM databases (http://bionet.ncpsb.org/batman-tcm/), which is a bioinformatics analysis tool for molecular mechanism of TCM to acquire predicted drug targets of each compound with scores no smaller than 20.[24] The canonical SMILES of active components were sent to the Swiss Target Prediction database (http://www.swisstargetprediction.ch/index.php) to predict protein targets of active components of AMC.[25] Then, duplications were removed from the

targets obtained from the above tools. Noteworthy, unified targets of Homo sapiens were kept for further study (Supplementary Table S2).

Renal Fibrosis Targets Predicting

Pathological targets for renal fibrosis were downloaded from GeneCards (https://www.genecards.org/). GeneCards is an online catalog of human genes and genetic diseases, which enables us to effectively navigate gene–disease linkages.[26] We got 197 genes with a relevance score more than 20, and details are described in Supplementary Table S3. All renal fibrosis-related genes provided by the GeneCards were then overlapped with identified putative targets of AMC and obtained 17 genes (Supplementary Table S4).

Construction of Compound-Target Network and Pathway Enrichment Analyses

The compound-target network was visualized using Cytoscape 3.7.2, an open source software platform for molecular interaction visualization (https://cytoscape.org/).[27] In the network diagram, nodes represent component, targets or pathways, and edges indicate the interactions among them. To further explore the functional annotation and signaling pathways that contributed to AMC in the treatment of renal fibrosis, gene ontology (GO) and Kyoto Encyclopedia of Genes and Genomes (KEGG) pathway enrichments of the obtained target networks were calculated by DAVID Bioinformatics Resources 6.8 (https://david.ncifcrf.gov/tools.jsp).[28]

Anti-Renal Fibrosis Targets of AMC and Function-Related Protein Interaction Network

The Search Tool for the Retrieval of Interacting Genes (STRING) database (https://string-db.org/) was employed to seek for the protein–protein interaction (PPI) data. "Multiple proteins" column was selected; the species was limited to "Homo sapiens". The proteins with high levels of connection were regarded as the important proteins for renal fibrosis treatment.

Contribution Indexes Calculation

The contribution index (CI) and network based efficacy (NE) were calculated to assess the contribution of each active component to the anti-renal fibrosis effect of AMC.[29] Equations are as follows:

$$NE(j) = \sum_{i=1}^{n} di$$

$$CI(j) = \frac{Cj \times NE(j)}{\sum_{i=1}^{n} Ci \times NE(i)}$$

In equation (a), j represents component, n is the number of targets connected with component j in component-target network (C-T network), d_i is the degree of target i connected with component j in target-pathway network (T-P network), and NE is the sum of component j connected with all targets' degree. In equation (b), ci is the number of renal fibrosis-related articles of ingredient i and all papers are obtained from PubMed Database. If the sum of CI for the top N components was more than 85%, these relevant N components were regarded as primary active components.

Reagents

Serum creatinine (Scr) and blood urea nitrogen (BUN) assay kits were purchased from Nanjing Jiancheng Biotech Co., Ltd. (Nanjing, Jiangsu, China). Enzyme-linked immunosorbent assay (ELISA) kit to determine the concentration of urinary albumin (UAlb) was purchased from JinYiBai Biological Technology Co., Ltd. (Nanjing, Jiangsu, China). Enhanced BCA Protein Assay Kit was obtained from Beyotime Institute of Biotechnology (Nanjing, Jiangsu, China). Anti-α-smooth muscle actin (α-SMA) antibody (ab32575) was purchased from Abcam (Cambridge, UK). Anti-vimentin (5741) antibody and anti-eNOS antibody (32,027) were obtained from Cell Signaling Technology (Beverly, MA, USA). Anti-collagen I (AF7001) was obtained from Affbiotech (Cincinnati, OH, USA). Anti-GAPDH (MB001) was purchased from Bioworld Technology (St. Louis Park, MN, USA). The IRDye (680RD or 800CW)-labeled secondary antibodies were purchased from LI-COR Biotechnology (Lincoln, NE, USA). ChamQ SYBR qPCR Master Mix (Low ROX Premixed) (Q331-02) and RNA isolater Total RNA Extraction Reagent (R401-01) were purchased from Vazyme Biotech Co., Ltd. (Nanjing, Jiangsu, China). All the inorganic chemicals were from Sigma-Aldrich (St. Louis, MO, USA).

Preparation of AMC

AMC was kindly provided by Jiangsu Suzhong Pharmaceutical Group Co., Ltd. Briefly, the dried corolla of *A. manihot* was extracted by 18-fold volumes of 75% ethanol (w/v) under reflux successively for 1 hour. The extract was filtered and then evaporated to produce a dry

extract powder under vacuum at 60°C. Ethanol extract powder was dissolved in ddH_2O to the desired concentrations before each experiment.

5/6 Nephrectomy and AMC Administration

The investigation was executed in accordance with the guidelines for the care and use of laboratory animals, after approval of the protocol by the Animal Ethics Committee of China Pharmaceutical University. Male Institute of Cancer Research (ICR) mice (body weight 22~26 g) purchased from the Comparative Medicine Center, Yangzhou University were housed in vivarium with controlled temperature (22±2°C) and humidity (50 ±10%), 12/12 hour light/dark cycle provided, with ad libitum access to food and water.

After arrival and acclimatization for a week, mice were anesthetized with pentobarbital sodium (70 mg/kg) and subjected to subtotal nephrectomy, ie, ablation of 2/3rds of renal parenchyma of the left side. One week later, right sided uninephrectomy was performed. Sham mice were operated on in parallel. On day 3 after the second operation, the mice with remnant kidneys were randomized into four groups: receiving vehicle (ddH_2O, n=10) or AMC (dissolved in ddH_2O at three doses of 0.15, 0.5, and 1.5 g/kg, for each dosage n=10). The dosage of AMC was normalized by body surface area to approximate human equivalence.[30] At the end of week 8, mice were housed in metabolic cages for 24 hours to collect urine and the blood was sampled from the ophthalmic veins. All of the animals were killed by cervical dislocation and the remnant kidneys were harvested, and processed for histological, Western blotting evaluation, or RNA isolation.

Scr, BUN, and UAlb Assay

Scr and BUN levels were quantitatively examined using Scr and BUN assay kits according to the manufacturer's instruction. UAlb was determined by an ELISA assay using a mouse UAlb quantification kit according to the manufacturer's instruction.

Histologic Examination of Renal Tissues

For the evaluation of renal histology, kidneys were perfused with ice-cold PBS and then stored in 10% phosphate buffered formalin. After embedding in resin, 4-μm thick sections were cut and stained with hematoxylin and eosin (H&E) or Masson's trichrome. Light microscope images were photographed using a Nanozoomer whole slide scanner (NanoZoomer 2.0 RS, Hamamatsu, Japan). Kidney injury score was graded on a scale from 0–4, as described previously.[31] In short, the glomerular number, tubular atrophy and degeneration, interstitial inflammation, and fibrous hyperplasia were semiquantitatively scored by pathologists who was blind with respect to the experimental data as follows: 0=none, 1=10%, 2=11–25%, 3=26–45%, 4=46–75%.

Western Blotting Analysis

Snap-frozen renal samples were homogenized in RIPA Lysis Buffer including 100 mg/mL PMSF. After incubation for 30 minutes on ice, the samples were centrifuged for 15 minutes at 12,000 rpm, and the supernatants were collected and assayed for protein content using Enhanced BCA Protein Assay Kit. An equal amount of protein extracts (40 μg) was analyzed by standard SDS-PAGE, transferred onto a nitrocellulose membrane, blocked with 5% milk and incubated with anti-α-SMA antibody (1:1000, Abcam), anti-collagen I antibody (1:1000, Affbiotech), anti-vimentin antibody (1:1000, Cell Signaling Technology), anti-PI3K antibody (1:1000, Cell Signaling Technology), anti-phospho-PI3K antibody (1:1000, Bioworld Technology), anti-Akt antibody (1:1000, Cell Signaling Technology), anti-phospho-Akt antibody (1:1000, Cell Signaling Technology), and anti-GAPDH (1:10,000, Bioworld Technology) overnight at 4°C. After several washes, membranes were incubated with the IRDye (680RD or 800CW)-labeled secondary antibodies (1:10,000) for 1 hour at room temperature, washed, and visualized using the LI-COR Odyssey Infrared Imaging System (LI-COR Biotechnology, Lincoln, NE, USA). Densitometry was carried out using LI-COR Odyssey Infrared Imaging System application software (version 2.1, LI-COR Biotechnology).

RNA Extraction and Analyses

Total RNA was extracted from renal tissues using RNA isolater Total RNA Extraction Reagent (Vazyme Biotech) according to the manufacturer's instructions. The concentration and the purity of RNA were measured spectrophotometrically using Nano-100 (Allsheng, Hangzhou, Zhejiang, China). mRNA transcript levels of α-SMA, collagen I, and vimentin were amplified with ChamQ SYBR qPCR Master Mix (Low ROX Premixed) (Vazyme Biotech). GAPDH was used as the endogenous control to normalize the amount of cDNA added to each reaction (ΔCT), and the mean ΔCT of control samples was used as

the calibrator to calculate the ΔΔCT. Quantitation of each transcript was by the comparative CT method. In this method, the relative quantity of target mRNA, normalized to the endogenous control and relative to the calibrator, is equal to $2^{-\Delta\Delta CT}$. Each experiment was carried out in triplicate at least twice; the results are expressed as means ±SEM of representative triplicates. Primer sequences were as follows: α-SMA, forward 5′-GTGATCACCATCGGGAATGA-3′, reverse 5′-CAGCAATGCCTGGGTACATG-3′; vimentin, forward 5′-GATCGATGTGGACGTTTCCAA-3′, reverse 5′-ATACTGCTGGCGCACATCAC-3′; collagen, forward 5′-AACCCCAAGGAGAAGAAGCA-3′, reverse 5′-AGCGTGCTGTAGGTGAATCG-3′, GAPDH, forward 5′- CAGGGCTGCCTTCTCTTGTG-3′, reverse 5′-GATGGTGATGGGTTTCCCGT-3′.

Statistical Analysis

Statistical significance was evaluated by the One-way ANOVA and, where appropriate, a Dunnett′s multiple comparison test. For all analyses, values of $P<0.05$ were regarded as statistically significant. Results were expressed as the mean±SEM.

Results

Potential active components and targets of AMC against renal fibrosis

In this work, caffeic acid, quercetin, stigmasterol, α-spinasterol, 9.12-octadecadienoic acid, and β-sitosterol are selected with OB≥30% and DL≥0.18. In addition, myricetin, quercetin-7-*O*-*β*-*D*-glucoside, quercetin-3-*O*-robinobioside, hyperoside, isoquercitrin, gossypetin-8-*O*-*β*-*D*-glucuronide, quercetin-3′-*O*-*β*-*D*-glucoside, and rutin are manually supplemented through a text-mining so that they are regarded as the main components in AMC with high content and superior pharmacological activity (Supplementary Table S1).[21,22] The 14 components from AMC result in 671 targets. After removing the duplicate targets, 248 non-repetitive potential targets were identified (Figure 1 and Supplementary Table S2).

The abovementioned targets were intersected with 197 target genes for renal fibrosis obtained in GeneCards (relevance scores more than 20). In the end, 17 genes were identified as targets of 14 components from AMC against renal fibrosis, including *MET*, *ACE*, *TNF*, *TERT*, *IL6*, *VEGFA*, *PIK3CA*, *MMP1*, *MMP9*, *EGFR*, *TLR4*, *IL2*, *FGF2*, *HNF4A*, *NR3C2*, *INSR*, and *ELANE* (Supplementary Table S4). These 17 identified target genes were used for further enrichment calculation and protein interaction analysis.

Enrichment Analysis of Candidate Targets for AMC Treating Renal Fibrosis

GO function and KEGG pathway enrichment analysis were carried out using the 17 recognized targets. The results revealed that AMC acted on renal fibrosis by regulating multiple biological processes (BP) ($P<0.01$), and the top five of them were positive regulation of nitric oxide biosynthetic process, MAP kinase activity, smooth muscle cell proliferation, ERK1 and ERK2 cascade and protein kinase B signaling, respectively (Figure 2A and Supplementary Table S5). Depending on the outcomes of cellular component (CC) analysis, extracellular region, extracellular space, cell surface, external side of plasma membrane, and receptor complex are the main terms (Figure 2B and Supplementary Table S6). As shown in Figure 2C and Supplementary Table S7, the top five molecular function (MF) included endopeptidase activity, cytokine activity, protein tyrosine kinase activity, growth factor activity and transmembrane receptor protein tyrosine kinase activity. KEGG pathway enrichment results revealed that the top five relevant pathways involved in AMC protection against renal fibrosis was proteoglycans in cancer, PI3K-Akt signaling pathway, HIF-1 signaling pathway, Chagas disease and pathways in cancer (Figure 2D and Supplementary Table S8).

Function-Related Protein Interaction Network

The highest 10 target genes with a high degree of connectivity (score≥10) were selected as the hub genes for AMC treating renal fibrosis (Figure 3). The hub genes, which might play critical roles in the progression of renal fibrosis, were growth factors (VEGFA, FGF2, EGFR, and MET), inflammatory factors (IL6, TNF, and IL2), and fibrotic matrix protein (MMP9). In the hub genes, VEGFA is considered as the most important one, which has 15 edges connected to other genes. The connectivity degrees of FGF2, IL6, EGFR, and MMP9 are 14, 14, 12, and 12, respectively (Figure 3B).

Component-Target-Pathway Network Analysis

A component-target-pathway network was conducted to visualize the complex relationship among all bioactive components, targets, and enriched signal pathways (Figure 4). All components are interconnected with multiple targets,

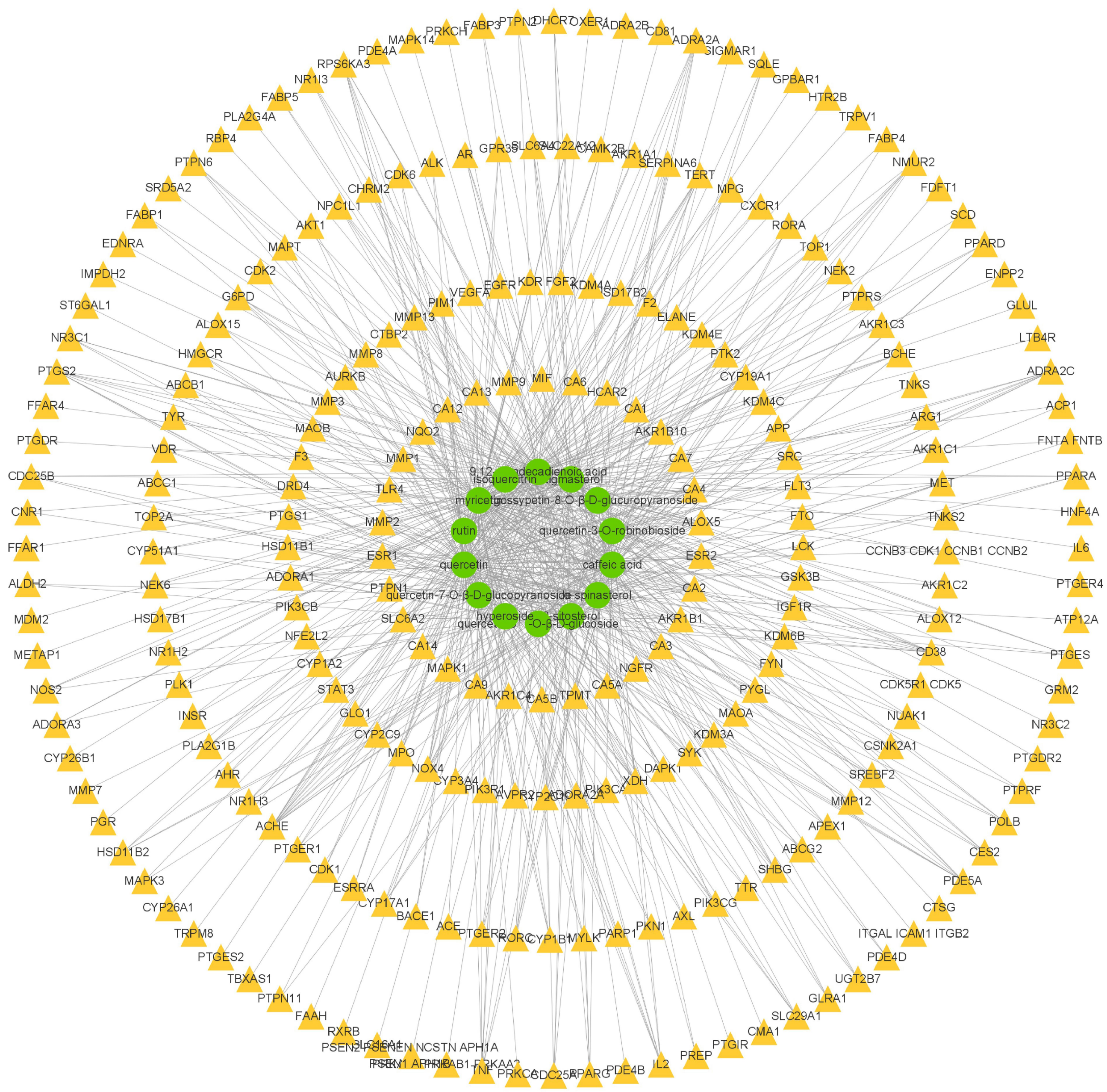

Figure 1 The compound-target network for AMC active components and corresponding targets. The green circles represent components, while the yellow triangles represent gene targets. A component and a target node are linked if the protein is targeted by the corresponding component.

especially caffeic acid (degree=8), quercetin (degree=6), 9.12-octadecadienoic acid (degree=4), and myricetin (degree=5). All targets were mapped to 40 enriched KEGG pathways. The results indicated that the PI3K-Akt signaling pathway exhibited the highest number of target connections (degree=9).

Based on the component-target-pathway network and literature, a CI of every active component was calculated to further screen the active components. The sum of CIs of quercetin, caffeic acid, 9.12-octadecadienoic acid, and myricetin are 85.86%, that is more than 85% (Figure 5 and Supplementary Table S9). So, these four components are recognized as the main effective compounds to the anti-renal fibrosis effect of AMC.

AMC Ameliorated Renal Function and Renal Fibrosis in the Remnant Kidney Model

Scr, BUN, and UAlb are the key markers indicating the kidney injury/dysfunction. 3 days after 5/6 nephrectomy, the levels of Scr, BUN, and UAlb significantly increased compared to the

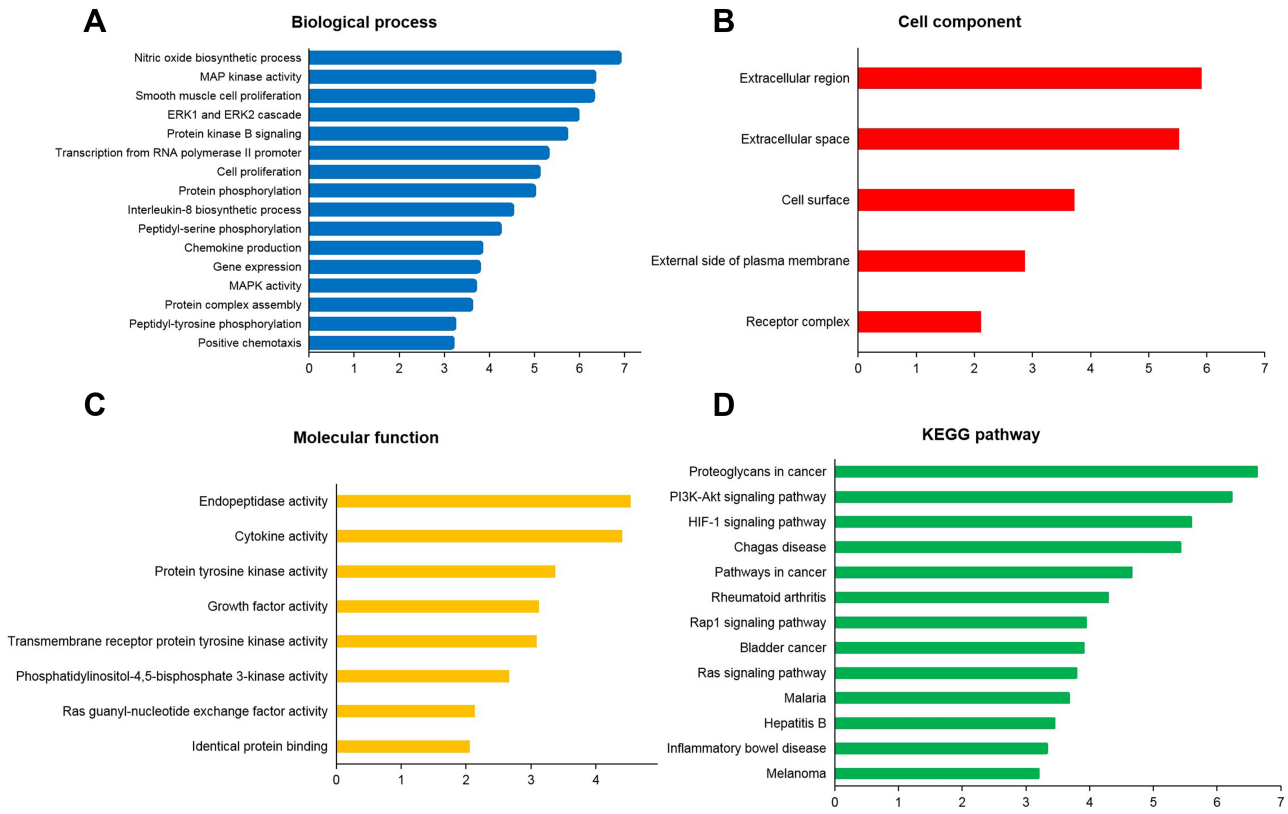

Figure 2 GO and KEGG analyses of targets from bioinformatics data. (**A**) Biological process analysis of targets; (**B**) Cell component analysis of targets; (**C**) Molecular function analysis of targets; (**D**) KEGG pathways of target genes. Database showed the remarkably enriched terms (P<0.01). The x-axis values were calculated as –log(P).

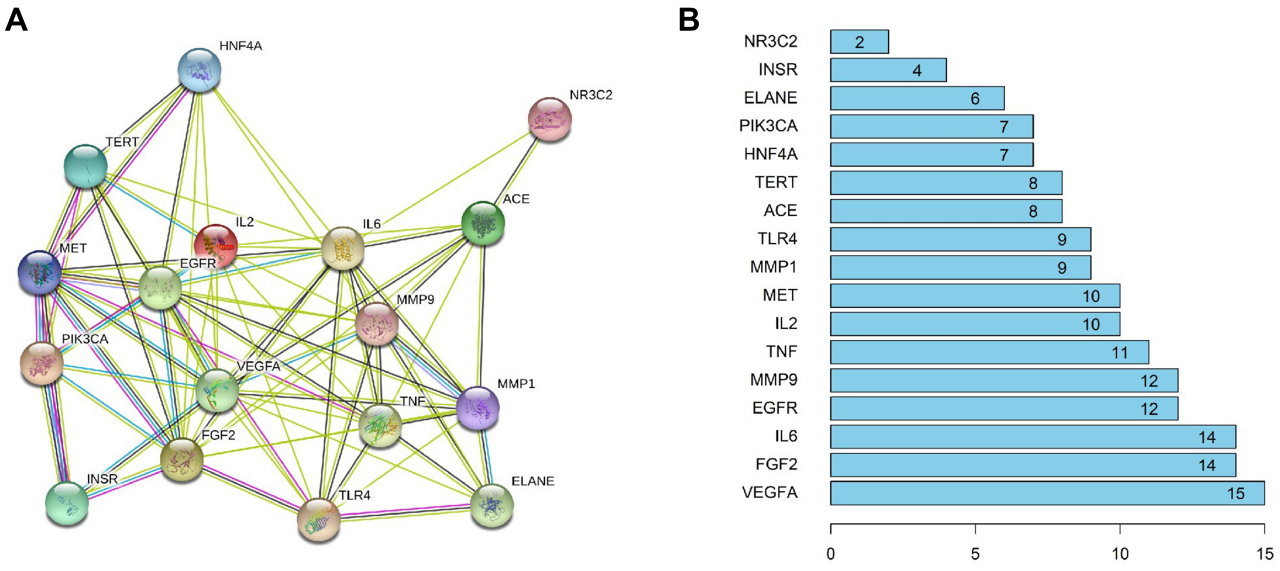

Figure 3 Protein–protein interaction (PPI) network of AMC for the treatment of renal fibrosis. (**A**) Network nodes represent proteins, and edges represent protein–protein associations. (**B**) The score of genes in PPI network, the higher the score, the more important the protein.

sham group. The changes of these physiological indexes indicated the impaired glomerular filtration function which demonstrated the 5/6 nephrectomy model was successfully established. Compared to the model group, AMC administration for 8 consecutive weeks dose-dependently decreased the levels of Scr, BUN, and UAlb, respectively (Figure 6).

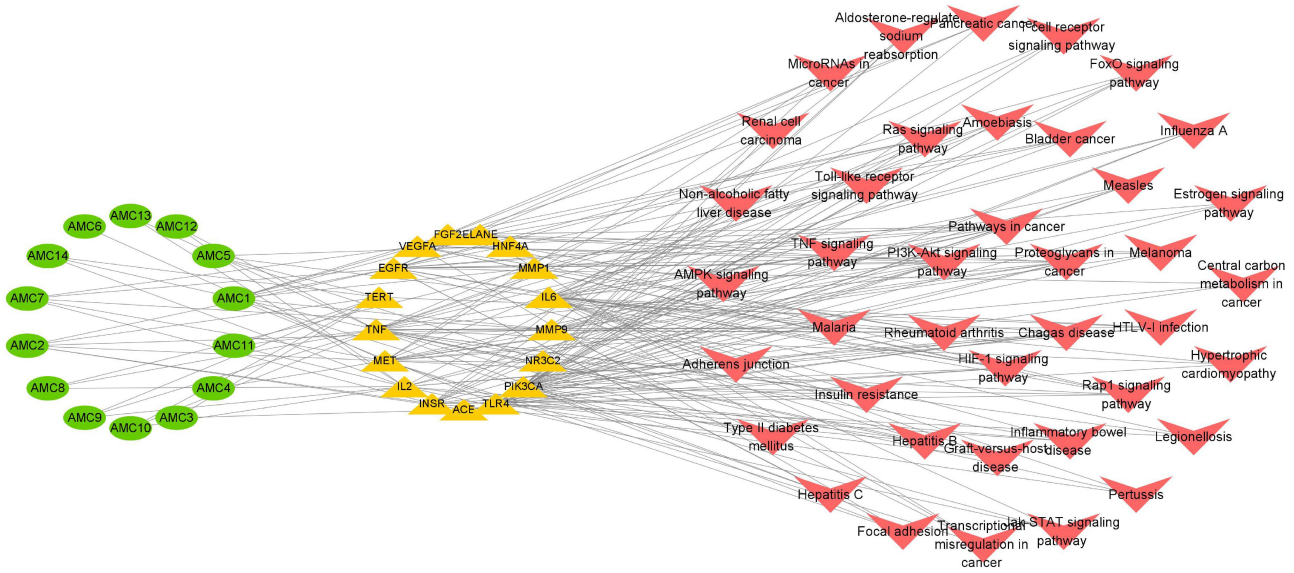

Figure 4 The component-target-pathway network for AMC against renal fibrosis. Green circles represent active ingredients in AMC. Yellow triangles represent common targets of AMC and renal fibrosis. Red arrows represent KEGG enriched signaling pathways.

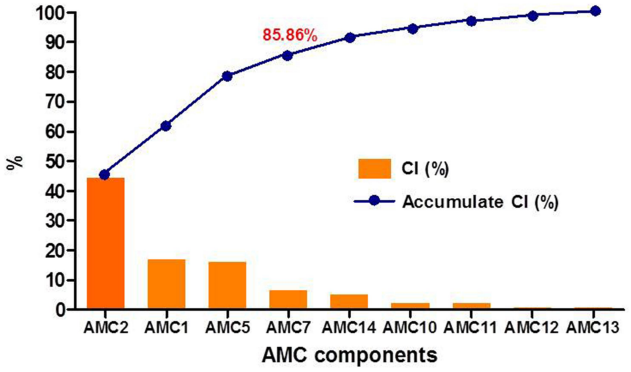

Figure 5 The CI and accumulative CI of active components in AMC. The sum of CIs for the top four components including AMC2 (quercetin), AMC1 (caffeic acid), AMC5 (9,12-octadecadienoic acid), and AMC7 (myricetin) was more than 85%. AMC3 (stigmasterol), AMC4 (α-spinasterol), AMC6 (β-sitosterol), AMC8 (quercetin-7-O-β-D-glucopyranoside), AMC9 (quercetin-3-O-robinobioside), AMC10 (hyperoside), AMC11 (isoquercitrin), AMC12 (gossypetin-8-O-β-D-glucuropyranoside), AMC13 (quercetin- 3′-O-β-D-glucoside), and AMC14 (rutin).

Histopathological examination of the remnant kidney was evaluated by H&E staining and Masson's trichrome staining, and the results showed that 5/6 nephrectomized mice developed significant inflammation infiltration, mesangial expansion, tubular atrophy and dilatation, glomerular sclerosis, and moderate interstitial fibrosis (Figure 7). The semi-quantification score of kidney injury showed 5/6 nephrectomy increased the score from 0.08±0.20 to 3.00±0.84 (P<0.001, n=4), and after administration of AMC, the scores significantly decreased to 1.83±0.26 (0.5 g/kg, P<0.05, n=4), and 1.20±0.57 (1.5 g/kg, P<0.01, n=4), respectively. Masson's trichrome staining demonstrated a visible increase of collagen deposition areas in the remnant kidney model (Figure 7). AMC treatment significantly alleviated the severity of glomerular sclerosis and interstitial fibrosis (Figure 7). In accordance with the histopathological results, Western blotting analysis revealed that 5/6 nephrectomized mice displayed 1.8-, 2.4-, and 12.6-fold increases in protein expressions of α-SMA, vimentin, and collagen I, respectively, which were markedly attenuated by AMC treatment in a dose-dependent manner (Figure 8 and supplementary figure). Consistent with the protein expression levels, 5/6 nephrectomy significantly increased the mRNA levels of α-SMA, vimentin, and collagen I to 2.2-, 2.4-, and 2.8-fold of their respective sham controls, and AMC administration reversed the 5/6 nephrectomy induced changes (Figure 8). Taken together, these data demonstrated that AMC displayed a protective effect against kidney fibrosis in 5/6 nephrectomized mice.

AMC Suppressed the PI3K-Akt-eNOS Signaling Pathway and ERK1/2 Target in 5/6 Nephrectomized Mice

KEGG pathway enrichment analysis and GO enrichment analysis predicted that the PI3K-Akt-eNOS signaling pathway was involved in AMC protection against renal fibrosis. We therefore investigated the key proteins expressions of the PI3K-Akt-eNOS pathway in 5/6 nephrectomized mice. The total expression levels of Akt and PI3K remained almost the same while the phosphorylated levels of PI3K and Akt were significantly increased to 1.61- and 3.67-fold of their respective sham controls after 5/6

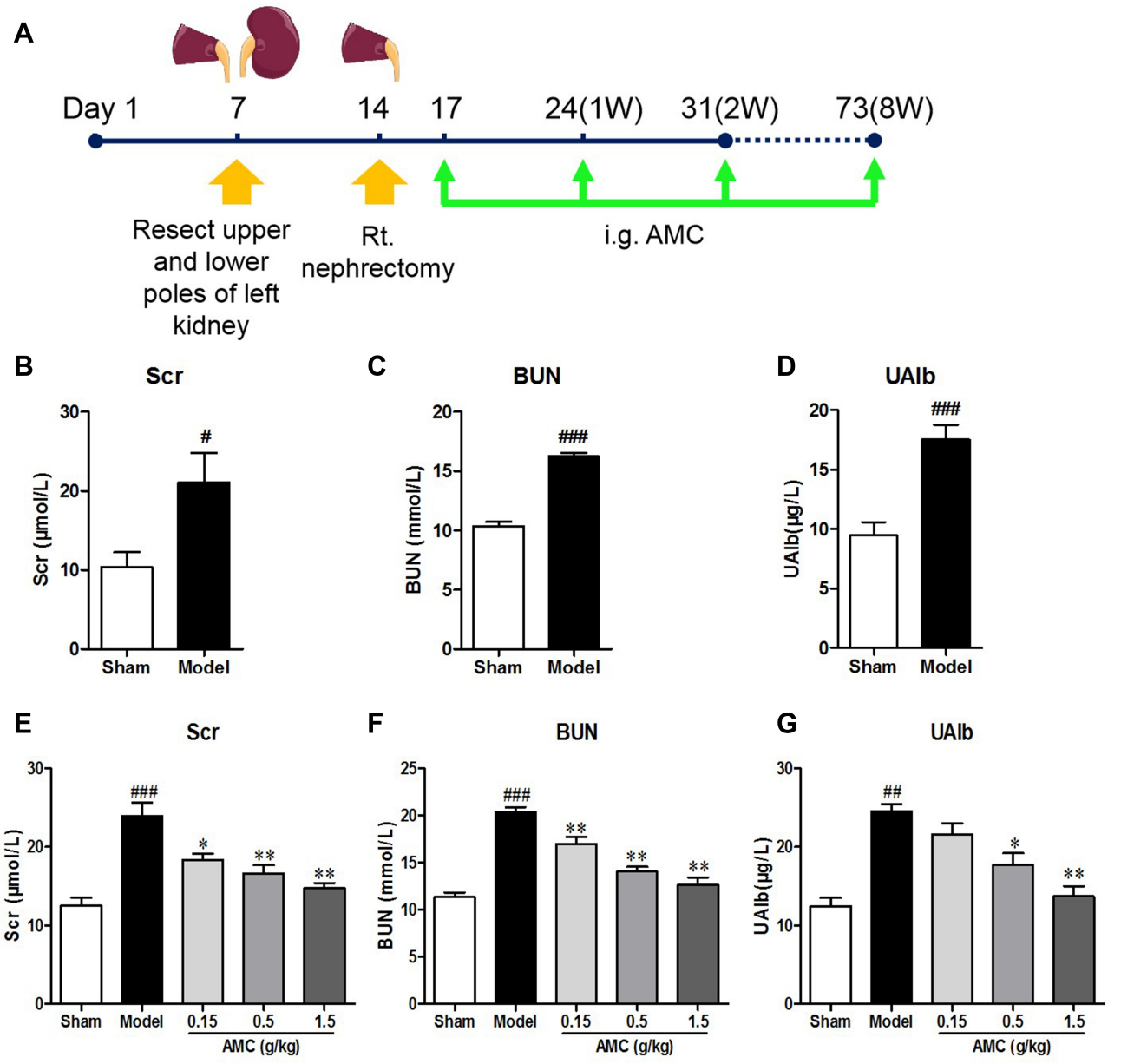

Figure 6 Experimental procedure, confirmation of kidney injury, and AMC administration. (**A**) Schema of mouse two-stage reduction in renal mass model (5/6 nephrectomy) and AMC administration protocol; (**B**–**D**) 5/6 nephrectomy increased the levels of Scr, BUN, and UAlb levels at 3 days after the second surgery (day 17). (**E**–**G**) Effects of AMC treatment on levels of Scr, BUN, and UAlb in 5/6 nephrectomized mice. $^{\#}P<0.05$, $^{\#\#}P<0.01$, $^{\#\#\#}P<0.001$, model group versus sham group; $^{*}P<0.05$, $^{**}P<0.01$, AMC group versus model group, data are presented as means ± SEM (n=10).

nephrectomy (Figure 9A and B). In addition, 5/6 nephrectomy markedly increased the expression of eNOS to 2.03-fold of the sham group mice (Figure 9C). AMC treatment significantly attenuated 5/6 nephrectomy induced phosphorylation levels of PI3K and Akt and the eNOS expression (Figure 9A–C and supplementary figure). The GO enrichment analysis for biological process revealed that MAP kinase activity and ERK1 and ERK2 cascade were related to a reno-protective effect of AMC. Therefore, the expressions of ERK1/2 were detected. Total expression level of ERK1/2 showed a slight increase after 5/6 nephrectomy compared to the sham group ($P>0.05$). The phosphorylation level of ERK1/2 was significantly increased to 1.7-fold of the sham group after 5/6 nephrectomy, and AMC administration reversed the change of the expression level of p-ERK1/2 (Figure 9D).

Discussion

Renal fibrosis is the common outcome of most progressive kidney diseases, irrespective of the causes, and closely

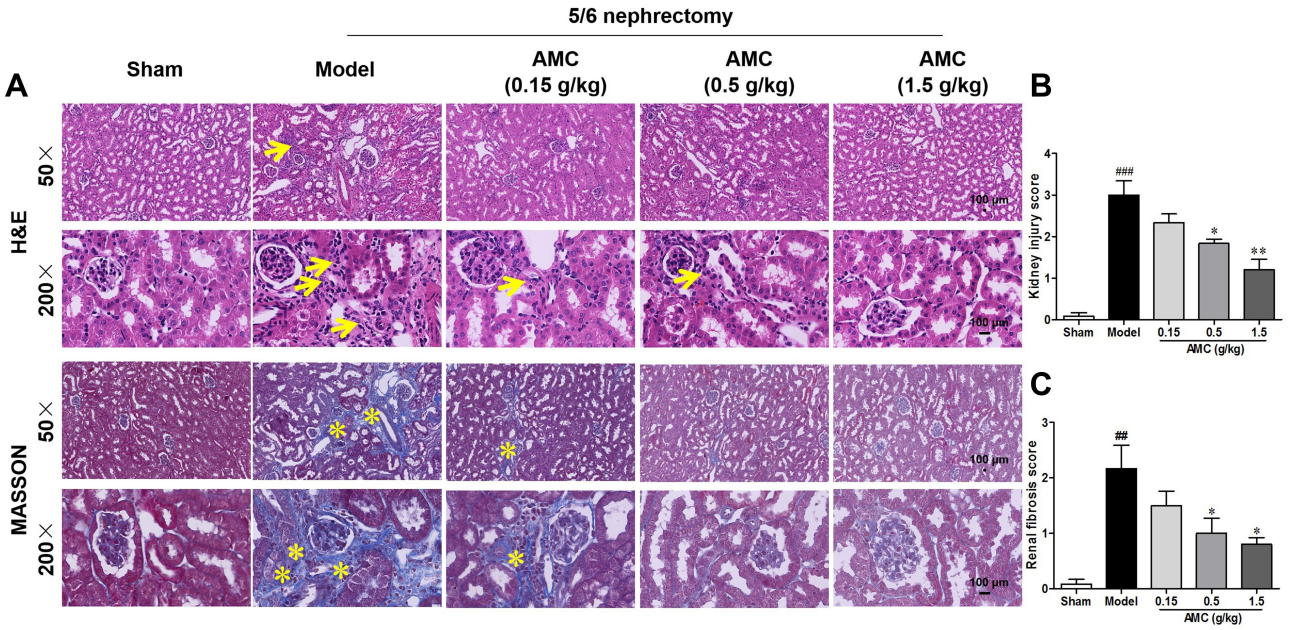

Figure 7 AMC suppressed inflammation filtration and collagen deposition in mice after 5/6 nephrectomy. (**A**) Representative images of H&E staining and the Masson's trichrome staining at 50× and 200× magnifications. Yellow arrows indicated the inflammatory infiltration or swelling of the kidney tissues. Yellow asterisks indicated the fibrotic tissues. Scale bar=100 μm for sections. (**B**–**C**) Quantitative analysis of H&E staining and Masson's trichrome staining. $^{\#\#}P<0.01$, $^{\#\#\#\#}P<0.001$, model group versus sham group; $^{*}P<0.05$, $^{**}P<0.01$, AMC group versus model group, data are presented as means±SEM (n=4).

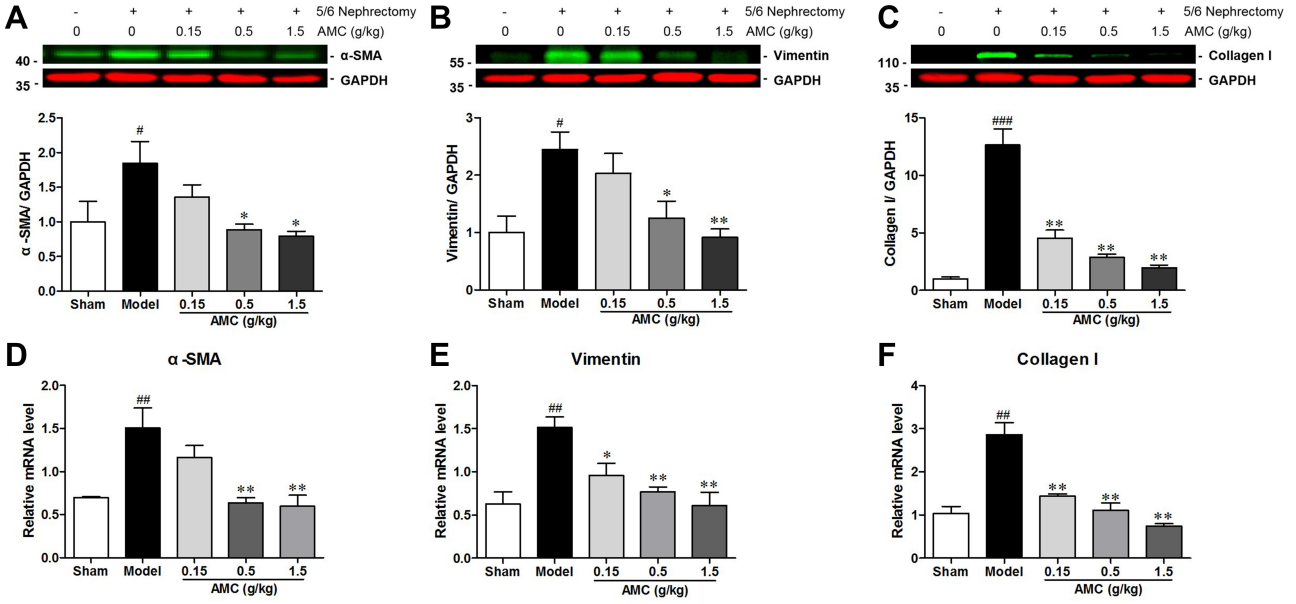

Figure 8 AMC suppressed renal fibrosis in mice after 5/6 nephrectomy. (**A**–**C**) Note representative immunoblots and quantification of the levels of α-SMA, vimentin, and collagen I. (**D**–**F**) mRNA levels of α-SMA, vimentin, and collagen I on week 8 after 5/6 nephrectomy determined by quantitative reverse transcriptase polymerase chain reaction. $^{\#}P<0.05$, $^{\#\#}P<0.01$, $^{\#\#\#\#}P<0.001$, model group versus sham group; $^{*}P<0.05$, $^{**}P<0.01$, AMC group versus model group, data are presented as means±SEM (n=3).

correlates with the deterioration of kidney function.[32] Reduction of renal mass by 5/6 nephrectomy effectively decreased the nephron number, and resulted in elevated pressure, permeation, and filtration for remnant nephrons. The persistent overload caused the remaining 1/6 kidney to be unable to maintain a homeostasis of internal environment, and eventually led to an ongoing loss of normal tissue structure.[33] Currently, the 5/6 nephrectomized model, characterized by gradual renal function loss and progressive renal scarring, has been recognized as a classic model with the

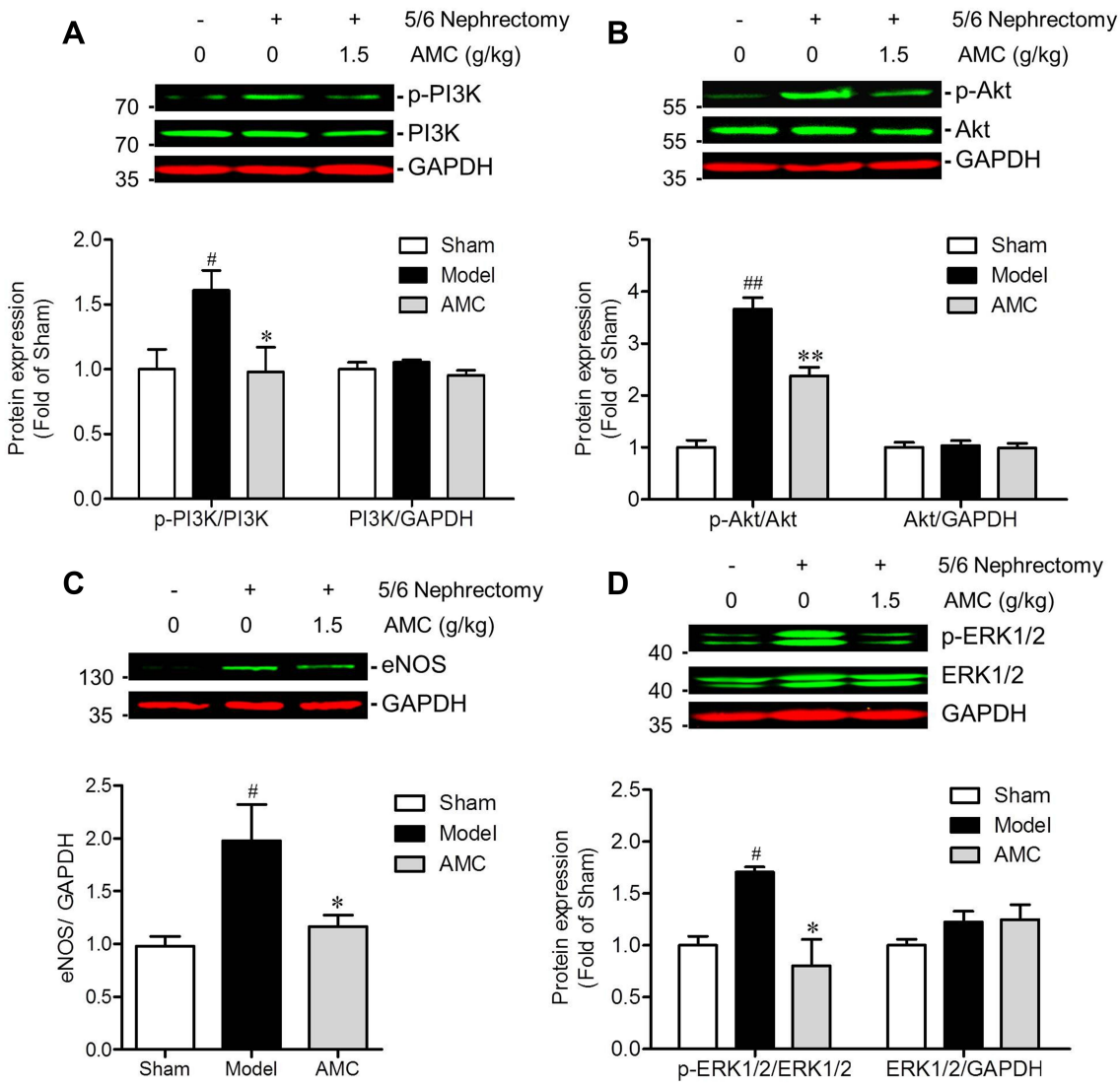

Figure 9 AMC treatment regulates PI3K-Akt-eNOS signaling pathway and ERK1/2 target in 5/6 nephrectomy induced renal fibrosis mice. Representative western blots and quantification of the levels of total and phosphorylated PI3K (**A**), Akt (**B**), and ERK1/2 (D) expression and the expression of eNOS (**C**) in sham, model and AMC treated groups. $^{\#}P < 0.05$, $^{\#\#}P < 0.01$, model group versus sham group; $^{*}P < 0.05$, $^{**}P < 0.01$, AMC group versus model group, data are presented as means ± SEM (n = 3).

optimal relevance to human CKD. It has been widely used to investigate the efficacy and mechanism of the test drug on CKD.[34,35] In the present study, we used a 5/6 nephrectomized mice model to observe the therapeutic effect and explore the potential mechanism of AMC against 5/6 nephrectomy-induced renal fibrosis combined with a network pharmacology approach.

First, Scr, BUN, and UAlb concentrations are measured as biomarkers for detecting renal injury. The appearance of excessive protein in urine was mainly due to negative charge barrier destruction.[36] Decreased glomerular filtration rate caused by macromolecular proteins filtration resulted in decreased filtration of Scr and BUN. In this study, oral administration of AMC for 8 consecutive weeks dose-dependently decreased the levels of Scr, BUN, and UAlb, respectively, indicating the protective effect on kidney injury/dysfunction in 5/6 nephrectomized mice.

Second, histologic examination revealed that 5/6 nephrectomized mice with AMC treatment exhibited significant improvement of renal fibrosis as evidenced by the reduced deposition of extracellular matrix (α-SMA, vimentin, and collagen I). Based on the histological structure, renal fibrosis usually divided into glomerulosclerosis, interstitial fibrosis, and arteriosclerosis.[37] In the diabetic nephropathy model and adriamycin nephropathy mice, podocytes are the primary targets and glomerular fibrosis is a common feature.[38,39] Our results indicated that collagen deposition is found in glomerular, tubulointerstitial, and perivascular at 8

weeks after 5/6 nephrectomy. Therefore, AMC had a comprehensive protection effect on renal fibrosis.

Third, In order to explore the bioactive components and potential pharmacological mechanisms of AMC in treating renal fibrosis, network pharmacology, as a novel research method for Chinese herbal formulas, was applied.[13,14] In this work, all targets of reported compounds from AMC were intersected with renal fibrosis associated genes, resulting in 17 potential targets, mainly from flavonoids and organic acids. According to the contribution indexes calculation results, quercetin, caffeic acid, 9.12-octadecadienoic acid, and myricetin are identified as the key active components. It is reported that quercetin could largely ameliorate the progression of kidney interstitial fibrosis and prevent the EMT of renal tubular proximal epithelial cells.[40,41] Caffeic acid possesses antifibrotic effects possibly through inhibiting AngII, TGF-β, and Smad3 signaling pathways.[42,43] 9.12-octadecadienoic acid, also named linoleic acid, is the most highly consumed polyunsaturated fatty acid found in the human diet, and showed a superior effect on modulating inflammation, fibrosis, and oxidative stress following obstructive renal injury.[44,45] In addition, myricetin was reported to inhibit diabetes-induced renal dysfunction and fibrosis.[22,46]

GO enrichment analysis revealed a nitric oxide biosynthetic process, MAP kinase activity, smooth muscle cell proliferation, as well as ERK1 and ERK2 cascade are the main biological process of AMC in the treatment of renal fibrosis. EMT of renal tubular proximal epithelial cells and proliferation and activation of resident fibroblasts remains the major route for the generation of myofibroblasts in renal fibrosis.[32] AMC was predicted to possess a protective effect on both myofibroblast resources. Reduced synthesis of endothelial nitric oxide synthase and NO result in endothelial cells impairment and excessive fibrosis.[47] In an adriamycin-induced renal injury model, total extracts of *A. manihot* flower showed potent suppression of activated ERK1/2 compared with MAPK activity,[48] which are consistent with our predicted results. As for KEGG pathway enrichment analysis, proteoglycans in cancer, the PI3K-AKT signaling pathway, and the HIF-1 signaling pathway are closely related to AMC in the application of renal fibrosis. It is known that EMT plays an important role in the development of both cancer and renal fibrosis, so the predicted result, proteoglycans in cancer, indicated that endothelial cells may be the effective cell. Phosphatidylinositol-3 kinases (PI3Ks) constitute a lipid kinase family and generate phosphatidylinositol-3,4,5-trisphosphate (PI(3, 4, 5)P3), which is a second messenger essential for the translocation of Akt from the cytoplasm to the inner surface of the cell membrane.[49] Akt, the serine/threonine kinase, is a well-characterized effector of PI3K and its deregulation plays a crucial role in the pathogenesis of renal fibrosis.[50] Increased activation of the PI3K-Akt pathway was detected in obstructed kidneys with an increased amount of interstitial extracellular matrix deposition.[51,52] High glucose/hypoxic-induced EMT of tubular epithelial cells also accompanied an increased level of Akt phosphorylation.[53] Our results indicated that the levels of p-PI3K and p-Akt, as well as the expression of eNOS were significantly increased in remnant kidneys. Oral administration of AMC markedly decreased 5/6 nephrectomy induced the phosphorylation levels of PI3K, Akt, ERK1/2, and the expression of eNOS along with the decrease in fibrosis markers α-SMA, vimentin, and fibronectin. And those data are in accordance with published results that Huangkui capsule inhibited the phosphorylation of Akt and alleviates the early glomerular pathological changes in diabetic nephropathy.[9,21]

Last, the hub genes, including growth factors (VEGFA, FGF2, EGFR, and MET), inflammatory factors (IL6, TNF, and IL2), and fibrotic matrix protein (MMP9), selected from the PPI network, exhibited high correlation with AMC against renal fibrosis. VEGF is a key mediator of normal and abnormal angiogenesis. The loss of tubular VEGF expression closely correlated with the severity of tubular cells loss.[54] FGF2 displays a potent capacity to induce tubulo-epithelial cell plasticity and its expression is significantly increased in fibrotic kidney.[55] EGFR is activated after renal damage, and plays a role in regulating renal inflammation, cell growth, and fibrosis.[56] MET is a hepatocyte growth factor receptor (HGF). The decrease in endogenous HGF augments susceptibility to the onset of renal tubular cells fibrosis.[57] IL6, TNF, and IL2 are important inflammatory factors during renal fibrosis.[32] MMP-9 is detrimental in renal interstitial fibrogenesis through digesting tubular basement membrane and in turn to promotion of EMT.[58] Above all, these hub genes are associated EMT and AMC plays a major role in inhibiting the EMT process of renal fibrosis.

Conclusions

In summary, we demonstrated the protective effect of AMC in a 5/6 nephrectomy model using ICR mice. Integrated network pharmacology analysis and pharmacological evaluation were applied to predict and verify the mechanism of *Abelmoschus manihot* (L.) Medik on 5/6 nephrectomy induced kidney fibrosis, possibly through inhibiting the PI3K-Akt-eNOS signaling pathway and

targeting ERK1/2. This study might provide a candidate from natural products for the treatment of renal fibrosis.

Abbreviations

ADME, absorption, distribution, metabolism, and excretion; AMC, corolla of *Abelmoschus manihot* (L.) Medik.; *A. manihot, Abelmoschus manihot* (L.) Medik.; α-SMA, anti-α-smooth muscle actin; BP, biological processes; BUN, blood urea nitrogen; CC, cellular component; CI, contribution index; CKD, chronic kidney disease; DL, drug-likeness; ELISA, enzyme-linked immunosorbent assay; EMT, epithelial-mesenchymal transition; GO, gene ontology; H&E, hematoxylin and eosin; ICR, Institute of Cancer Research; KEGG, Kyoto Encyclopedia of Genes and Genomes; MAPK, mitogen-activated protein kinase; MF, molecular function; NE, network based efficacy; OB, oral bioavailability; PI3Ks, phosphatidylinositol-3 kinases; PPI, protein–protein interaction; STRING, Search Tool for the Retrieval of Interacting Genes; Scr, serum creatinine; TCMs, traditional Chinese medicines; TCMSP, traditional Chinese medicine systems pharmacology database; UAlb, urinary albumin.

Funding

This research was funded by National Natural Science Foundation of the People's Republic of China (grant number 81872974).

Disclosure

The authors report no conflicts of interest for this work.

References

1. Murphy D, McCulloch CE, Lin F, et al. Trends in prevalence of chronic kidney disease in the United States. *Ann Intern Med*. 2016;165(7):473. doi:10.7326/M16-0273
2. Hill NR, Fatoba ST, Oke JL, et al. Global prevalence of chronic kidney disease - a systematic review and meta-analysis. *PLoS One*. 2016;11(7):e0158765. doi:10.1371/journal.pone.0158765
3. Zhou D, Liu Y. Renal fibrosis in 2015: understanding the mechanisms of kidney fibrosis. *Nat Rev Nephrol*. 2016;12(2):68–70. doi:10.1038/nrneph.2015.215
4. Fleck C, Appenroth D, Jonas P, et al. Suitability of 5/6 nephrectomy (5/6NX) for the induction of interstitial renal fibrosis in rats - Influence of sex, strain, and surgical procedure. *Exp Toxicol Pathol*. 2006;57(3):195–205. doi:10.1016/j.etp.2005.09.005
5. Chen D, Feng Y, Cao G, Zhao Y. Natural products as a source for antifibrosis therapy. *Trends Pharmacol Sci*. 2018;39(11):937–952. doi:10.1016/j.tips.2018.09.002
6. Geng X, Zhong D, Su L, Yang B. Preventive and therapeutic effect of *Ganoderma* (Lingzhi) on renal diseases and clinical applications. *Adv Exp Med Biol*. 2019;1182:243–262. doi:10.1007/978-981-32-9421-9_10
7. Zhang L, Li P, Xing C, et al. Efficacy and safety of *Abelmoschus manihot* for primary glomerular disease: a prospective, multicenter randomized controlled clinical trial. *Am J Kidney Dis*. 2014;64(1):57–65. doi:10.1053/j.ajkd.2014.01.431
8. Carney EF. Antiproteinuric efficacy of *A. manihot* superior to losartan. *Nat Rev Nephrol*. 2014;10(6):300. doi:10.1038/nrneph.2014.63
9. Wu W, Hu W, Han W, et al. Inhibition of Akt/mTOR/p70S6K signaling activity with Huangkui capsule alleviates the early glomerular pathological changes in diabetic nephropathy. *Front Pharmacol*. 2018;9. doi:10.3389/fphar.2018.00443
10. Han W, Ma Q, Liu Y, et al. Huangkui capsule alleviates renal tubular epithelial-mesenchymal transition in diabetic nephropathy via inhibiting NLRP3 inflammasome activation and TLR4/NF-κB signaling. *Phytomedicine*. 2019;57:203–214. doi:10.1016/j.phymed.2018.12.021
11. Zhang R, Zhu X, Bai H, Ning K. Network pharmacology databases for traditional Chinese medicine: review and assessment. *Front Pharmacol*. 2019;10:123. doi:10.3389/fphar.2019.00123
12. Li S, Zhang B. Traditional Chinese medicine network pharmacology: theory, methodology and application. *Chin J Nat Med*. 2013;11(2):110–120. doi:10.1016/S1875-5364(13)60037-0
13. Wu R, Jiang B, Li H, et al. A network pharmacology approach to discover action mechanisms of Yangxinshi Tablet for improving energy metabolism in chronic ischemic heart failure. *J Ethnopharmacol*. 2020;246:112227. doi:10.1016/j.jep.2019.112227
14. Wei S, Niu M, Wang J, et al. A network pharmacology approach to discover active compounds and action mechanisms of San-Cao Granule for treatment of liver fibrosis. *Drug Des Devel Ther*. 2016;10:733–743. doi:10.2147/DDDT.S96964
15. Hao M, Ji D, Li L, et al. Mechanism of *Curcuma wenyujin* rhizoma on acute blood stasis in rats based on a UPLC-Q/TOF-MS metabolomics and network approach. *Molecules*. 2019;24(1):82. doi:10.3390/molecules24010082
16. Xia KY, Zhang CL, Cao ZY, et al. Chemical constituents from *Corolla abelmoschi*. *Strait Pharm J*. 2019;31(9):58–61. doi:10.3969/j.issn.1006-3765.2019.09.018
17. Xu X, Zhang W, Huang C, et al. A novel chemometric method for the prediction of human oral bioavailability. *Int J Mol Sci*. 2012;13(6):6964–6982. doi:10.3390/ijms13066964
18. Ma C, Wang L, Xie XQ. GPU accelerated chemical similarity calculation for compound library comparison. *J Chem Inf Model*. 2011;51(7):1521–1527. doi:10.1021/ci1004948
19. Liu J, Mu J, Zheng C, et al. Systems-pharmacology dissection of traditional Chinese medicine compound Saffron formula reveals multi-scale treatment strategy for cardiovascular diseases. *Sci Rep-UK*. 2016;6(1):19809. doi:10.1038/srep19809
20. Xu X, Bi J, Ping L, Li P, Li F. A network pharmacology approach to determine the synergetic mechanisms of herb couple for treating rheumatic arthritis. *Drug Res Devel Ther*. 2018;12:967–979. doi:10.2147/DDDT.S161904
21. Mao Z, Shen S, Wan Y, et al. Huangkui capsule attenuates renal fibrosis in diabetic nephropathy rats through regulating oxidative stress and p38MAPK/Akt pathways, compared to α-lipoic acid. *J Ethnopharmacol*. 2015;173:256–265. doi:10.1016/j.jep.2015.07.036
22. Cai H, Su S, Qian D, et al. Renal protective effect and action mechanism of Huangkui capsule and its main five flavonoids. *J Ethnopharmacol*. 2017;206:152–159. doi:10.1016/j.jep.2017.02.046
23. Kim S, Thiessen PA, Bolton EE, et al. PubChem substance and compound databases. *Nucleic Acids Res*. 2016;44(D1):D1202–D1213. doi:10.1093/nar/gkv951
24. Liu Z, Guo F, Wang Y, et al. BATMAN-TCM: a bioinformatics analysis tool for molecular mechANism of traditional Chinese medicine. *Sci Rep-UK*. 2016;6(1). doi:10.1038/srep21146
25. Daina A, Michielin O, Zoete V. SwissTargetPrediction: updated data and new features for efficient prediction of protein targets of small molecules. *Nucleic Acids Res*. 2019;47(W1):W357–W364. doi:10.1093/nar/gkz382

26. Stelzer G, Rosen N, Plaschkes I, et al. The GeneCards suite: from gene data mining to disease genome sequence analyses. *Curr Protoc Bioinformatics*. 2016;54(1). doi:10.1002/cpbi.5
27. Demchak B, Hull T, Reich M, et al. Cytoscape: the network visualization tool for GenomeSpace workflows. *F1000Research*. 2014;3:151. doi:10.12688/f1000research.4492.2
28. Jiao X, Sherman BT, Huang DW, et al. DAVID-WS: a stateful web service to facilitate gene/protein list analysis. *Bioinformatics*. 2012;28(13):1805–1806. doi:10.1093/bioinformatics/bts251
29. Yue S, Xin L, Fan Y, et al. Herb pair Danggui-Honghua: mechanisms underlying blood stasis syndrome by system pharmacology approach. *Sci Rep-UK*. 2017;7(1). doi:10.1038/srep40318
30. Nair AB, Jacob S. A simple practice guide for dose conversion between animals and human. *J Basic Clin Pharm*. 2016;7(2):27–31. doi:10.4103/0976-0105.177703
31. Gu L, Wang Y, Yang G, et al. *Ribes diacanthum* Pall (RDP) ameliorates UUO-induced renal fibrosis via both canonical and non-canonical TGF-β signaling pathways in mice. *J Ethnopharmacol*. 2018;231:302–310. doi:10.1016/j.jep.2018.10.023
32. Liu Y. Cellular and molecular mechanisms of renal fibrosis. *Nat Rev Nephrol*. 2011;7(12):684–696. doi:10.1038/nrneph.2011.149
33. Kujal P, Vernerov Z. 5/6 nephrectomy as an experimental model of chronic renal failure and adaptation to reduced nephron number. *Cesk Fysiol*. 2008;57(4):104.
34. Kren S, Hostetter TH. The course of the remnant kidney model in mice. *Kidney Int*. 1999;56(1):333–337. doi:10.1046/j.1523-1755.1999.00527.x
35. Leelahavanichkul A, Yan Q, Hu X, et al. Angiotensin II overcomes strain-dependent resistance of rapid CKD progression in a new remnant kidney mouse model. *Kidney Int*. 2010;78(11):1136–1153. doi:10.1038/ki.2010.287
36. Haraldsson BR, Nystr MJ, Deen WM. Properties of the glomerular barrier and mechanisms of proteinuria. *Physiol Rev*. 2008;88 (2):451–487. doi:10.1152/physrev.00055.2006
37. Djudjaj S, Boor P. Cellular and molecular mechanisms of kidney fibrosis. *Mol Aspects Med*. 2019;65:16–36. doi:10.1016/j.mam.2018.06.002
38. Wang Y, Wang YP, Tay YC, Harris DC. Progressive Adriamycin nephropathy in mice: sequence of histologic and immunohistochemical events. *Kidney Int*. 2000;58(4):1797–1804. doi:10.1046/j.1523-1755.2000.00342.x
39. Gurley SB, Clare SE, Snow KP, et al. Impact of genetic background on nephropathy in diabetic mice. *Am J Physiol Renal Physiol*. 2006;290(1):F214–22. doi:10.1152/ajprenal.00204.2005
40. Ren J, Li J, Liu X, et al. Quercetin inhibits fibroblast activation and kidney fibrosis involving the suppression of mammalian target of rapamycin and β-catenin Signaling. *Sci Rep-UK*. 2016;6(1). doi:10.1038/srep23968
41. Lu Q, Ji X, Zhou Y, et al. Quercetin inhibits the mTORC1/p70S6K signaling-mediated renal tubular epithelial–mesenchymal transition and renal fibrosis in diabetic nephropathy. *Pharmacol Res*. 2015;99:237–247. doi:10.1016/j.phrs.2015.06.006
42. Chuang S, Kuo Y, Su M. KS370G, a caffeamide derivative, attenuates unilateral ureteral obstruction-induced renal fibrosis by the reduction of inflammation and oxidative stress in mice. *Eur J Pharmacol*. 2015;750:1–7. doi:10.1016/j.ejphar.2015.01.020
43. Mia MM, Bank RA. The pro-fibrotic properties of transforming growth factor on human fibroblasts are counteracted by caffeic acid by inhibiting myofibroblast formation and collagen synthesis. *Cell Tissue Res*. 2016;363(3):775–789. doi:10.1007/s00441-015-2285-6
44. Ogborn MR, Nitschmann E, Bankovic-Calic N, et al. Dietary conjugated linoleic acid reduces PGE2 release and interstitial injury in rat polycystic kidney disease. *Kidney Int*. 2003;64(4):1214–1221. doi:10.1046/j.1523-1755.2003.00215.x
45. Whelan J, Fritsche K. Linoleic Acid. *Adv Nutr*. 2013;4(3):311–312. doi:10.3945/an.113.003772
46. Yang Z, Wang H, Wang Y, et al. Myricetin attenuated diabetes-associated kidney injuries and dysfunction via regulating nuclear factor (erythroid derived 2)-like 2 and nuclear factor-κB Signaling. *Front Pharmacol*. 2019;10. doi:10.3389/fphar.2019.00647
47. Osmanagic-Myers S, Kiss A, Manakanatas C, et al. Endothelial progerin expression causes cardiovascular pathology through an impaired mechanoresponse. *J Clin Invest*. 2019;129(2):531–545. doi:10.1172/JCI121297
48. Li W, He W, Xia P, et al. Total extracts of *Abelmoschus manihot* L. attenuates Adriamycin-induced renal tubule injury via suppression of ROS-ERK1/2-mediated NLRP3 inflammasome activation. *Front Pharmacol*. 2019;10:567. doi:10.3389/fphar.2019.00567
49. Cantley LC. The phosphoinositide 3-kinase pathway. *Science*. 2002;296(5573):1655–1657. doi:10.1126/science.296.5573.1655
50. Lan A, Du J. Potential role of Akt signaling in chronic kidney disease. *Nephrol Dial Transpl*. 2015;30(3):385–394. doi:10.1093/ndt/gfu196
51. Rodrguez-Pe AB, Grande MT, Eleno NL, et al. Activation of Erk1/2 and Akt following unilateral ureteral obstruction. *Kidney Int*. 2008;74 (2):196–209. doi:10.1038/ki.2008.160
52. Dou F, Liu Y, Liu L, et al. Aloe-Emodin ameliorates renal fibrosis via inhibiting PI3K/Akt/mTOR signaling pathway in vivo and in vitro. *Rejuvenation Res*. 2019;22(3):218–229. doi:10.1089/rej.2018.2104
53. Zhang X, Liang D, Fan J, et al. Zinc attenuates tubulointerstitial fibrosis in diabetic nephropathy via inhibition of HIF through PI-3K signaling. *Biol Trace Elem Res*. 2016;173(2):372–383. doi:10.1007/s12011-016-0661-z
54. Kang D, Johnson RJ. Vascular endothelial growth factor: a new player in the pathogenesis of renal fibrosis. *Curr Opin Nephrol*. 2003;12:43–49. doi:10.1097/01.mnh.0000049814.98789.10
55. Guan X, Nie L, He T, et al. Klotho suppresses renal tubulo-interstitial fibrosis by controlling basic fibroblast growth factor-2 signalling. *J Pathol*. 2014;234(4):560–572. doi:10.1002/path.4420
56. Rayego-Mateos S, Rodrigues-Diez R, Morgado-Pascual JL, et al. Role of epidermal growth factor receptor (EGFR) and its ligands in kidney inflammation and damage. *Mediat Inflamm*. 2018;2018:1–22. doi:10.1155/2018/8739473
57. Matsumoto K, Nakamura T. Hepatocyte growth factor: renotropic role and potential therapeutics for renal diseases. *Kidney Int*. 2001;59(6):2023–2038. doi:10.1046/j.1523-1755.2001.00717.x
58. Wang X, Zhou Y, Tan R, et al. Mice lacking the matrix metalloproteinase-9 gene reduce renal interstitial fibrosis in obstructive nephropathy. *Am J Physiol Renal*. 2010;299(5):F973–F982. doi:10.1152/ajprenal.00216.2010

Drug Design, Development and Therapy

Dovepress

Publish your work in this journal

Drug Design, Development and Therapy is an international, peer-reviewed open-access journal that spans the spectrum of drug design and development through to clinical applications. Clinical outcomes, patient safety, and programs for the development and effective, safe, and sustained use of medicines are a feature of the journal, which has also been accepted for indexing on PubMed Central. The manuscript management system is completely online and includes a very quick and fair peer-review system, which is all easy to use. Visit http://www.dovepress.com/testimonials.php to read real quotes from published authors.

Submit your manuscript here: https://www.dovepress.com/drug-design-development-and-therapy-journal